Inorganic Chemistry

Communication

pubs.acs.org/IC

Magnetic Circular Dichroism and Electronic Structure of $[Re_2X_4(PMe_3)_4]^+$ (X = Cl, Br)

Diana Habel-Rodriguez,[†] Frederic Poineau,[‡] Erik V. Johnstone,[‡] Kenneth R. Czerwinski,[‡] Alfred P. Sattelberger,*[,‡,§] and Martin L. Kirk*[,†]

[†]Department of Chemistry and Chemical Biology, The University of New Mexico, MSC03 2060, 1 University of New Mexico, Albuquerque, New Mexico 87131-0001, United States

[‡]Department of Chemistry, University of Nevada Las Vegas, Las Vegas, Nevada 89154, United States

[§]Energy Engineering and Systems Analysis Directorate, Argonne National Laboratory, Lemont, Illinois 60439, United States

Supporting Information

ABSTRACT: Magnetic circular dichroism (MCD) and electronic absorption spectroscopies have been used to probe the electronic structure of the classical paramagnetic metal−metal-bonded complexes $[Re_2X_4(PMe_3)_4]^+$ (X = Cl, Br). A violation of the MCD sum rule is observed that indicates the presence of ground-state contributions to the MCD intensity. The *z*-polarized $\delta \rightarrow \delta^*$ band in the near-IR is formally forbidden in MCD but gains intensity through a combination of ground- and excited-state mechanisms to yield a positive *C* term.

The most interesting and most studied feature in the electronic absorption spectra of quadruply metal−metal-bonded complexes [i.e., dinuclear species with a $\sigma^2\pi^4\delta^2$ ground-state (GS) configuration] is the lowest-energy, electric-dipole-allowed $\delta \rightarrow \delta^*$ transition.[1−3] The archetypal example of this type of complex is the storied octachlorodirhenate ion, $[Re_2Cl_8]^{2-}$, whose electronic structure and spectroscopy have been thoroughly investigated and analyzed.[4−10] In the late1970s, magnetic circular dichroism (MCD) measurements played an important role in the elucidation of the electronic structures of both $[Re_2Cl_8]^{2-}$ and its bromide analogue,[11] but the technique has not found widespread application in the study of other multiply metal−metal-bonded complexes since that time.[12] The room temperature MCD spectra of the *diamagnetic* $[Re_2X_8]^{2-}$ (X = Cl, Br) ions display very weak temperature-independent *B* terms for the lowest-energy $\delta \rightarrow \delta^*$ transition and strong, temperature-independent, derivative-shaped *A* terms for the dipole-allowed $X(\pi) \rightarrow \delta^*$ bands at higher energy.[11] Paramagnetic dinuclear complexes with $\sigma^2\pi^4\delta^2\delta^{*1}$ GS configurations and their attendant metal−metal bond orders of 3.5 would appear to be ideal candidates for spectroscopic investigations using MCD but, to the best of our knowledge, have not been examined with this technique. Herein we describe our initial studies on the $[Re_2X_4(PMe_3)_4]^+$ cations (X = Cl, Br),[13] which provide new insight into the electronic structures of this class of multiply metal−metal-bonded dimers.

The $Re_2X_4(PMe_3)_4$ dimers were prepared and purified by literature methods and oxidized in air to $[Re_2Cl_4(PMe_3)_4]PF_6$ (**1**) and $[Re_2Br_4(PMe_3)_4]PF_6$ (**2**) in a mixture of ether and acetonitrile using a slight deficiency of $[NO]PF_6$.[13] Isolated **1** and **2** were washed with toluene to remove the neutral parent compounds and stored under argon. The crystal structures of $Re_2Cl_4(PMe_3)_4$ and $[Re_2Cl_4(PMe_3)_4]^+$ have been reported,[14] the latter as the chloride[15] or perrhenate salt,[14] and the point symmetries of the $Re_2X_4P_4$ cores are D_{2d} (Figure 1). The room temperature electronic absorption and 5 K MCD spectra of **1** and **2** (Figure 2) display two prominent bands (A and B) between 6000 and 25000 cm^{-1}. The band in the near-IR (NIR) region of the electronic absorption spectrum ($\varepsilon \sim 4000\ M^{-1}\ cm^{-1}$) is assigned as the $\delta \rightarrow \delta^*$ transition (transition 1), in agreement with prior work on these ions[13] and the related complex $[Re_2Cl_4(PPr^n_3)_4]^+$.[16] The corresponding band in MCD is a positive, temperature-dependent *C* term that possesses a well-resolved vibrational fine structure. This $\delta \rightarrow \delta^*$ *C*-term band is of interest because it is *z*-polarized and is therefore formally forbidden in MCD.[17] The energy and intensity of the $\delta \rightarrow \delta^*$ transition directly probe the nature of the Re−Re δ and Re−L bonding interactions,[2] and the near-equivalent energies and intensities for this transition in **1** and **2** ($\Delta E \sim 200\ cm^{-1}$) indicate that there is a negligible difference in the δ bond order. Absorption bands for **1** and **2** show optical electronegativity[18] shifts to lower energy for **2**, with a greater degree of X → Re ligand-to-metal charge-transfer character in band B than in band A. The MCD dispersion in the region of band B is complex and is comprised of dominant positive and weaker negative temperature-dependent features.

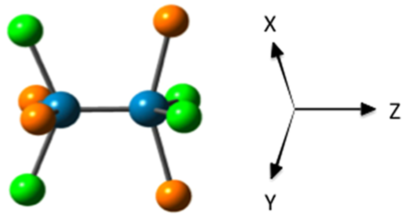

Figure 1. D_{2d} structure of the **1** core. Color code: Re, blue; Cl, green; P, orange.

Gaussian resolution of the electronic absorption spectra indicates that at least three transitions contribute to the intensity

Received: November 9, 2013
Published: January 17, 2014

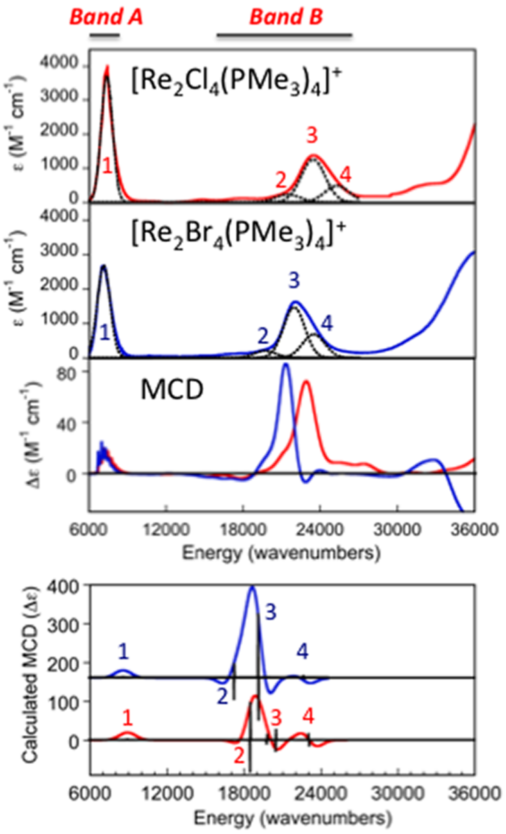

Figure 2. (Top) Experimental electronic absorption and MCD spectra for **1** (red) and **2** (blue). (Bottom) Computed MCD spectra for **1** (red) and **2** (blue). Note that the black lines give the relative computed MCD intensities.

of band B. Our time-dependent density functional theory (DFT) and MCD calculations[19−22] indicate that the complex MCD in the region of band B results from overlap and partial cancellation of multiple temperature-dependent MCD pseudo-*A* terms that derive from one-electron promotions involving doubly degenerate orbitals (Table 1). We assign transitions 2 and 3 as e → a_2 ($^2A \rightarrow {}^2E$) one-electron promotions from filled ligand orbitals (i.e., 31% Cl and 45% Cl for transitions 2 and 3, respectively) into the Re−Re δ^* orbital. Transition 4 is likely due to a one-electron promotion from the Re−Re δ orbital into the Re−Re π^* virtual orbital. Thus, the greater optical electronegativity shifts observed for band B compared to band A are consistent with a greater degree of halide character in the transitions that contribute to band B.

Table 1. Band Assignments for 1[a]

band	transition	energy (cm^{-1})	C-term	assignment
A	1	7300 (7100)	+ C	δ/X → δ^*/X
B	2	21300 (19700)	pseudo-*A*	X/P/π → δ^*/X
	3	23400 (21900)	pseudo-*A*	X/π → δ^*/X
	4	25300 (23400)	pseudo-*A*	δ/X → π^*

[a] [Re$_2$Br$_4$(PMe$_3$)$_4$]$^+$ data in parentheses.

The *xy*-polarized transitions that contribute to band B explain how the *z*-polarized $\delta \rightarrow \delta^*$ transition gains MCD intensity. Here, either the $^2B_1$ excited state (ES, |*J*⟩) or the $^2A_2$ GS (|*A*⟩) must mix with one or more *xy*-polarized ^2E ESs (|*K*⟩) by spin−orbit coupling (SOC; Figure 3).[17] In this manner, the *z*-polarized $^2A_2 \rightarrow {}^2B_1$ ($\delta \rightarrow \delta^*$) transition can acquire partial *x* or *y* character and display *C*-term MCD intensity. Typically, SOC between ESs will dominate because they are closer in energy to each other than to the GS (Figure 3).[17] However, the MCD spectra of **1** and **2** are dominated by positive features at energies <30000 cm^{-1}, indicating a violation of the MCD sum rule[17] and a GS mechanism contributing to the MCD intensity (Figure 3). Our MCD computations support this assertion and show that both ES and GS mechanisms[17,23] contribute to the observed positive *C*-term MCD associated with band A. Specifically, the GS mechanism dominates for **1** (52.8% GS vs 47.2% ES), and the ES mechanism dominates for **2** (40.4% GS vs 59.6% ES). This GS mechanism has also been suggested to contribute to the MCD intensity in plastocyanin[20] and the CuA site.[24]

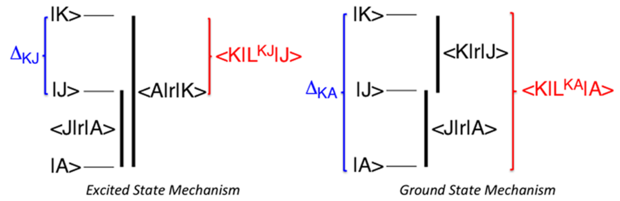

Figure 3. ES and GS contributions to the MCD intensity of band A. The Δ values are energy gaps between states, ⟨*i*|*r*|*j*⟩ are transition dipole integrals, and ⟨*i*|*L*^{kl}|*j*⟩ are spin−orbit matrix elements. The states |*A*⟩, |*J*⟩, and |*K*⟩ are defined in the text.

In summary, we have used a combination of electronic absorption and MCD spectroscopies, coupled with spectroscopic computations, to assign the dominant NIR and visible electronic transitions in **1** and **2**. This has allowed us to obtain a greater understanding of the electronic structure and bonding in these classical paramagnetic metal−metal-bonded complexes. To our knowledge, this is the first detailed MCD study of paramagnetic metal−metal dimers that probes the fundamental details of their electronic structure.

■ ASSOCIATED CONTENT

Ⓢ Supporting Information

ADF references, energies of the main progression-forming mode, computed transition energies, oscillator strengths, and MCD intensities. This material is available free of charge via the Internet at http://pubs.acs.org.

■ AUTHOR INFORMATION

Corresponding Authors
*E-mail: asattelberger@anl.gov.
*E-mail: mkirk@unm.edu.

Notes

The authors declare no competing financial interest.

■ ACKNOWLEDGMENTS

M.L.K. acknowledges NSF Grant CHE-1301142 for financial support. K.R.C. acknowledges an SISGR Grant (U.S. Department of Energy, Office of Science, Office of Basic Energy Sciences, under Contract 47824B) for financial support. We thank Prof. M. D. Hopkins (University of Chicago) and Dr. K. D. John (Los Alamos National Laboratory) for helpful suggestions on the synthesis and purification of **1** and **2**.

■ REFERENCES

(1) Trogler, W. C.; Gray, H. B. *Acc. Chem. Res.* **1978**, *11*, 232.

(2) Hopkins, M. D.; Gray, H. B.; Miskowski, V. M. *Polyhedron* **1987**, *6*, 705.
(3) Cotton, F. A. In *Multiple Bonds between Metal Atoms*, 3rd ed.; Cotton, F. A., Murillo, C. A., Walton, R. A., Eds.; Springer: New York, 2005.
(4) Cowman, C. D.; Gray, H. B. *J. Am. Chem. Soc.* **1973**, *95*, 8177.
(5) Cotton, F. A.; Frenz, B. A.; Stults, B. R.; Webb, T. R. *J. Am. Chem. Soc.* **1976**, *98*, 2768.
(6) Trogler, W. C.; Cowman, C. D.; Gray, H. B.; Cotton, F. A. *J. Am. Chem. Soc.* **1977**, *99*, 2993.
(7) Hay, P. J. *J. Am. Chem. Soc.* **1982**, *104*, 7007.
(8) Bursten, B. E.; Cotton, F. A.; Fanwick, P. E.; Stanley, G. G. *J. Am. Chem. Soc.* **1983**, *105*, 3082.
(9) Cotton, F. A.; Nocera, D. G. *Acc. Chem. Res.* **2000**, *33*, 483.
(10) Bursten, B. E.; Clayton, T. W. *J. Cluster Sci.* **1994**, *5*, 157.
(11) Cowman, C. D.; Trogler, W. C.; Gray, H. B. *Isr. J. Chem.* **1977**, *15*, 308.
(12) Mason, W. R. *A Practical Guide to Magnetic Circular Dichroism Spectroscopy*; John Wiley & Sons, Inc.: Hoboken, NJ, 2007.
(13) Root, D. R.; Blevins, C. H.; Lichtenberger, D. L.; Sattelberger, A. P.; Walton, R. A. *J. Am. Chem. Soc.* **1986**, *108*, 953.
(14) Cotton, F. A.; Jennings, J. G.; Price, A. C.; Vidyasagar, K. *Inorg. Chem.* **1990**, *29*, 4138.
(15) Cotton, F. A.; Dikarev, E. V.; Petrukhina, M. A. *Inorg. Chem. Commun.* **1999**, *2*, 28.
(16) Bursten, B. E.; Cotton, F. A.; Fanwick, P. E.; Stanley, G. G.; Walton, R. A. *J. Am. Chem. Soc.* **1983**, *105*, 2606.
(17) Neese, F.; Solomon, E. I. *Inorg. Chem.* **1999**, *38*, 1847.
(18) Jorgensen, C. K. *Mol. Phys.* **1963**, *6*, 43.
(19) Spin-unrestricted gas-phase geometry optimizations and MCD computations were performed at the DFT level using the Amsterdam Density Functional suite (*ADF 2012.01*).
(20) Seth, M.; Ziegler, T. *Inorg. Chem.* **2009**, *48*, 1793.
(21) Seth, M.; Ziegler, T. In *Advances in Inorganic Chemistry: Theoretical and Computational Inorganic Chemistry*; Van Eldik, R., Harvey, J., Eds.; Elsevier: New York, 2010; Vol. *62*, p 41.
(22) Seth, M.; Ziegler, T.; Autschbach, J. *J. Chem. Phys.* **2008**, *129*, 104105.
(23) Kirk, M. L.; Peariso, K. *Curr. Opin. Chem. Biol.* **2003**, *7*, 220.
(24) Xie, X.; Gorelsky, S. I.; Sarangi, R.; Garner, D. K.; Hwang, H. J.; Hodgson, K. O.; Hedman, B.; Lu, Y.; Solomon, E. I. *J. Am. Chem. Soc.* **2008**, *130*, 5194.